Proc. Indian Acad. Sci. (Chem. Sci.), Vol. 98, Nos 1 & 2, January 1987, pp. 1–12.

Neutron diffraction and optical studies of the ionic ferromagnet Rb_2CrCl_4 doped with Mg^{2+}, V^{2+} and Fe^{2+}

P J FYNE, M T HUTCHINGS[+] and P DAY*

Oxford University, Inorganic Chemistry Laboratory, South Parks Road, Oxford OX1 3QR, England

[+]Materials Physics Division, AERE Harwell, Didcot, Oxon OX11 ORA, England

Abstract. Powder and single crystal neutron diffraction and optical spectroscopy are used to study the effect of substituting non-magnetic (Mg^{2+}) or magnetic (V^{2+}, Fe^{2+}) cations on the Cr^{2+} sites in the ionic ferromagnet Rb_2CrCl_4. Comparison of powder neutron diffraction of Rb_2CrCl_4 and $Rb_2Cr_{0.73}Mg_{0.27}Cl_4$ shows that the latter still exhibits long range order at 4·2 K with the moments parallel to the basal plane. Single crystal neutron diffraction shows that substituting 11% Mg^{2+} lowers the Curie temperature by 19% and 3% V^{2+} lowers it by 6%. Analysis of satellite fine-structure near the exciton-magnon hot bands in the visible absorption spectra of crystals of Rb_2CrCl_4 doped with V^{2+} and Fe^{2+} leads to estimates of 6·6 K and 5·2 K for the Cr^{2+}-V^{2+} and Cr^{2+}-Fe^{2+} exchange constants.

Keywords. Neutron diffraction; ferromagnet; doped Rb_2CrCl_4.

1. Introduction

When a ferromagnet is diluted with non-magnetic ions the spin correlations are reduced and the Curie temperature T_c tends towards zero at a critical concentration of magnetic ions called the percolation limit, below which there are only finite clusters of magnetic ions. Rb_2CrCl_4 is an example of a two-dimensional square planar Heisenberg ferromagnet (Hutchings *et al* 1981) for which the theoretical percolation limit x is 0·59 (Shante and Kirkpatrick 1971). It is therefore of interest to observe the effect of increasing the concentration of both non-magnetic (Mg^{2+}) and magnetic (V^{2+}) dopant ions M^{2+} in $Rb_2Cr_xM_{1-x}Cl_4$. A convenient way to monitor T_c is to measure the temperature dependence of the magnetic intensity of a suitable reflection by single crystal neutron diffraction, though there is an upper limit to the concentration of dopant ions that can be incorporated into Rb_2CrCl_4 and still allow preparation of large crystals. In this paper we report measurements of T_c for crystals of composition $Rb_2Cr_{0.89}Mg_{0.11}Cl_4$ and $Rb_2Cr_{0.97}V_{0.03}Cl_4$. For higher concentrations of dopant ions, where only polycrystalline samples are available, powder neutron diffraction can still indicate the presence of magnetic order. However, the preferred moment direction is not so unambiguously defined as by a single crystal experiment. As well as reporting the powder neutron diffraction of $Rb_2Cr_{0.73}Mg_{0.27}Cl_4$ at 78 and 4·7 K we have measured and refined powder neutron diffraction profiles of Rb_2CrCl_4 itself for comparison. The magnetic structure of the latter has already been determined by single crystal neutron diffraction (Janke *et al* 1983) so it is of interest to see how clear an

*To whom all correspondence should be addressed.

indication of the moment orientation the powder data gives. We also give a brief account of this method of structure determination.

A further point of interest about Rb_2CrCl_4 is that it is unique among the small group of transparent ionic ferromagnets in having discrete optical absorption bands in the visible region. These bands have been studied in detail both theoretically (Harrop 1981) and experimentally (Janke *et al* 1982). They arise from magnon-exciton combination excitations via the 'hot-band' mechanism (Shinagawa and Tanabe 1971), which involves the coupling of an excitation created by photon absorption to simultaneous annihilation of a thermally populated magnon. Therefore, as the temperature is raised, the intensity of these bands increases with the thermal magnon population. We have shown (Wood *et al* 1982) that when Rb_2CrCl_4 is doped with Mn^{2+} the exciton-magnon bands develop satellite sidebands, whose energy separation from the parent absorption bands depends on the Cr^{2+}-Mn^{2+} exchange constant. Similar spectra of Rb_2CrCl_4 doped with V^{2+} and Fe^{2+} are reported here, together with the spectrum of a crystal doped with Mg^{2+}, which demonstrates that the sidebands arise only from magnetic impurities.

2. Experimental

Crystals of Rb_2CrCl_4 doped with Mg^{2+}, V^{2+} and Fe^{2+} were grown by the methods described previously (Walker *et al* 1982). A powder of composition $Rb_2Cr_{0\cdot73}Mg_{0\cdot27}Cl_4$ was prepared by quickly cooling a molten mixture of RbCl, $CrCl_2$ and $MgCl_2$ in a sealed silica ampoule. The ratio of Cr^{2+} to Mg^{2+} in the powder was determined by atomic absorption spectroscopy.

Powder neutron diffraction data were collected on the Dido Curran diffractometer at AERE Harwell using an incident neutron wavelength of 1·37 Å. The sample was contained in a vanadium can and mounted in a CT14 cryostat. Diffraction patterns were recorded at 4·2 K and above T_c. Scans of 2θ from 5° to 90° were employed with 0·1° steps and a counting time of 2 minutes.

The highest concentration of Mg^{2+} found in a single crystal boule was 11% in a Czochralski grown sample whose composition varied from 13% to 10% Mg^{2+} across a 0·75 cm section. The boule consisted of two major crystallites with axes sufficiently well-separated to be treated as distinct crystals. It was aligned on the crystal axes of the larger crystallite in a CT14 cryostat. At each temperature the (0, 0, 4) peak intensity was measured on the Dido MK VI 2 circle diffractometer at AERE Harwell using a neutron wavelength of 1·093 Å. The procedure employed was to carry out a scan of the crystal angle ω followed by an $\omega/2\theta$ scan, the maximum of the latter being taken as the intensity of the peak. This peak intensity was corrected for diffuse scattering and background, measured by making an $\omega/2\theta$ scan at (0, 0, 3·65). The highest concentration of V^{2+} which could be obtained in a single crystal with a small concentration gradient was 3%. The temperature variation of (0, 0, 4) intensity in a crystal of $Rb_2Cr_{0\cdot97}V_{0\cdot03}Cl_4$ was measured following the same procedure as that used for the Mg^{2+}-doped crystal.

Absorption spectra were measured with a McPherson RS10 high resolution double beam spectrophotometer equipped with an Oxford Instruments CF100 continuous flow helium cryostat.

3. Results and discussion

3.1 *Powder neutron diffraction: Rb_2CrCl_4 and $Rb_2Cr_{0.73}Mg_{0.27}Cl_4$*

The Rietveld refinement technqiue (Rietveld 1969) was employed to determine the nuclear and magnetic structures of pure and Mg^{2+} doped Rb_2CrCl_4. In this method one assumes that each Bragg diffraction peak is of Gaussian lineshape and fits the calculated profile $Y_i$calc to the measured profile $Y_i$obs at each value of the Bragg angle $2\theta_i \cdot Y_i$calc is expressed as

$$Y_i\,\text{calc} = tS_R^2 j_R L_R \frac{2(\ln 2)^{1/2}}{H_R(\pi)^{1/2}} \times \exp[-4\ln 2\{2\theta_i - 2\theta_R)/H_R\}]^2, \tag{1}$$

where $Y_i$calc is the calculated number of counts, S_R is the total structure factor (defined below) for reflection R, H_R is the full width of the peak at half height, L_R is the Lorentz factor, $2\theta_R$ is the calculated Bragg angle of the peak, t is the step width and j_R is the multiplicity of the reflection.

The angular dependence of the halfwidths of the diffraction peaks is expressed as

$$H_R^2 = U\tan^2\theta_R + V\tan\theta_R + W, \tag{2}$$

where U, V and W are the halfwidth parameters determined from the refinement.

The square of the total structure factor is given as

$$S_R^2 = (F_{N\text{calc}}^2 + F_{M\text{calc}}^2\sin^2\alpha)\exp[-2B\sin^2\theta_R/\lambda^2 + G\beta_R^2], \tag{3}$$

where F_N, F_M are the nuclear and magnetic structure factors, α is the angle between the reciprocal lattice vector and the moment direction, B is the overall isotropic temperature parameter, G is the preferred orientation parameter (a measure of the halfwidth of the assumed Gaussian distribution of the normals about the preferred orientation direction) and β is the acute angle between the scattering vector and the normal to the preferred direction of the crystallites.

For a centrosymmetric unit cell $F_{M\text{calc}}$ is expressed in terms of the magnetic vector K as

$$F_{M\text{calc}} = \sum_\phi \sum_j \sum_q f_j K_{\phi,j,q} \cos 2\pi(hx_{j,q} + ky_{j,q} + lz_{j,q}). \times\exp(-B_j\sin^2\theta_R/\lambda^2) \tag{4}$$

where f_j is the form factor, $K_{\phi,j,q}$ (in Bohr magnetons) is the component of the magnetic vector in the ϕ direction ($\phi = x, y, x$; cartesian axes), localised on the jth atom at the qth equivalent position. B_j is the individual isotropic temperature parameter for atom j. The magnetic vector can undergo rotation i.e.

$$\begin{pmatrix} K_{x,j,q} \\ K_{y,j,q} \\ K_{z,j,q} \end{pmatrix} = M_{j,q} \times \begin{pmatrix} K_x \\ K_y \\ K_z \end{pmatrix}, \tag{5}$$

where $M_{j,q}$ is the 3×3 rotation matrix describing the rotation of the magnetic vector of the jth atom at the qth equivalent position. $Y_i$obs is defined as the measured number of counts minus the background counts for the same preset monitor count.

The principle of the least squares refinement is to minimise R_p, (P = Profile) defined as

$$R_p = 100\times\sum_i \left| Y_i\text{obs} - \frac{1}{C}Y_i\text{calc}\right| \Big/ \sum_i Y_i\text{obs}. \qquad (6)$$

Other values obtained are

$$R_N = 100\times\sum_i \left| F^2_{N\text{obs},i} - \frac{1}{C}F^2_{N\text{calc},i}\right| \Big/ \sum F^2_{N\text{obs},i}\ , \qquad (7)$$

$$R_M = 100\times\sum_i \left| F^2_{M\text{obs},i} - \frac{1}{C}F^2_{M\text{calc},i}\right| \Big/ \sum_i F^2_{M\text{obs},i}\ , \qquad (8)$$

where C is the overall scale factor such that $Y_{\text{calc}} = CY_{\text{obs}}$.

The data were fitted using the 'Powder' suite of programmes mounted on the DEC 10 at E.R.C.C., Edinburgh.

Single crystal neutron diffraction studies of Rb_2CrCl_4 have shown that the crystals contain domains of two space groups *Acam* and *Bbcm*, corresponding to two alternative ways of packing the Jahn-Teller distorted layers. However, in a powder diffraction experiment the reflections from both domains occur at the same 2θ. Hence, the refinement of the powder data can be treated as a one-domain problem. In the present case the *Bbcm* space group was employed in the structure refinement because the orientation of the crystallographic c-axis coincides with that of the $I4$/mmm cell of the parent undistorted K_2NIF_4 lattice, and *Bbcm* notation is used for all (h, k, l) in this paper.

The results of the refinement for the nuclear only and the nuclear and magnetic structures are given in table 1. The coherent scattering lengths used were $b_{\text{Rb}} = 0{\cdot}71$, $b_{\text{Cr}} = 0{\cdot}352$, $b_{\text{Cl}} = 0{\cdot}96$, $b_{\text{Mg}} = 0{\cdot}52\times10^{-12}$ cm, (Bacon 1975). In the refinements the positional parameter of $C11(x)$ was not set equal to $C11(y)$ but both were allowed to vary independently.

Fit 1 (table 1) lists the parameters refined for Rb_2CrCl_4 at 78 K. This temperature is well above T_c (52 K, Hutchings *et al* 1981) and hence only the nuclear structure parameters were refined. Fits 2 to 4 list the refined nuclear and magnetic parameters for Rb_2CrCl_4 at 4·2 K where the $F_M$calc was calculated from the method used by Halpern and Johnson (1939). The magnetic moment was assumed to be localised in the $Cr^{2+}3d$ orbital and an isotropic $Cr^{2+}3d\,\langle j_0\rangle$ represented the form factor. An identity rotation matrix (5) operated at the Cr equivalent positions, thus assuming that the moments are all aligned parallel. In the fit an initial moment direction was chosen i.e. (K_x, K_y, K_z) and the components were varied.

Fit 2 lists the refined parameters when the moment is constrained along [010]. This fit is shown in figure 1 with low angle reflections indexed, and the weak (0, 0, 4) reflection used in the following section to monitor the magnetization of the doped compounds by single crystal neutron diffraction can just be detected. Fit 3

Table 1. Refinements of powder neutron diffraction data for Rb_2CrCl_4 (fits 1–4) and $Rb_2Cr_{0\cdot73}Mg_{0\cdot27}Cl_4$ (fits 5–6).

Fit number	1	2	3	4	5	6	Janke *et al* (1983) single crystal data refinements	
Temperature (K)	78	4·2	4·2	4·2	4·2	4·2	78	5.5
Initial spin direction	—	0, 1, 0	1, 0, 0	0, 0, 1	0, 1, 0	0, 0, 1	—	1, 1, 0 fixed
Rb (z)	0·3587(4)	0·3580(5)	0·3580(5)	0·3595(5)	0·3560(8)	0·3570(8)	0·3556(18)	0·3568(18)
Cl(2) (z)	0·1540(3)	0·1540(3)	0·1541(4)	0·1539(3)	0·1531(7)	0·1532(6)	0·1510(14)	0·1508(14)
Cl(1) (x)	0·2391(14)	0·2399(19)	0·2399(17)	0·2400(19)	0·2415(36)	0·2417(36)	0·2341(1)	0·2346(1)
Cl(1) (y)	0·2366(11)	0·2343(11)	0·2343(11)	0·2354(13)	0·2344(21)	0·2349(22)	0·2342(1)	0·2346(1)
Rb (B)[Å²]	1·07(17)	0·49(23)	0·48(23)	0·76(23)	0·50(34)	0·57(33)	0·47(9)	0·37(5)
Cr (B)[Å²]	0·33(26)	0·83(38)	0·81(37)	1·11(41)	0·96(53)	1·11(53)	0·49(16)	0·57(8)
Cl(2) (B)[Å²]	1·21(14)	1·20(19)	1·21(19)	1·02(16)	0·86(24)	0·83(22)	1·43(9)	0·59(4)
Cl(1) (B)[Å²]	1·02(8)	0·85(11)	0·85(10)	1·06(11)	0·69(13)	0·74(13)	0·48(3)	0·36(3)
K_x	—	0·0	3·8(1)	0·0	0·0	0·0	—	—
K_y	—	3·8(1)	0·0	0·0	2·5(3)	0·0	—	—
K_z	—	0·0	0·0	3·1(1)	0·0	2·38(2)	—	—
Moment [μ_B]*	—	3·8(1)	3·8(1)	3·1(1)	2·5(3)	2·4(2)	—	3·12(34)
a [Å]	7·211(2)	7·196(2)	7·197(2)	7·197(2)	7·141(6)	7·143(6)	7·183(18)	7·193(18)
b [Å]	7·185(2)	7·173(2)	7·173(2)	7·172(2)	7·114(6)	7·112(6)	7·183(2)	7·193(18)
c [Å]	15·698(2)	15·702(2)	15·701(2)	15·701(2)	15·761(6)	15·760(6)	15·67(4)	15·72(4)
Preferred orientation parameter	0·175(6)	0·183(7)	0·187(7)	0·164(7)	0·035(11)	0·022(11)	—	—
$R_{Nuclear}$ (%)	10·31	7·79	7·82	8·81	10·71	10·75	—	—
$R_{Magnetic}$ (%)	—	10·84	10·72	10·91	16·96	17·73	—	—
$R_{Profile}$ (%)	10·31	10·20	10·20	10·91	16·39	17·32	—	—

* Mean moment per metal ion site

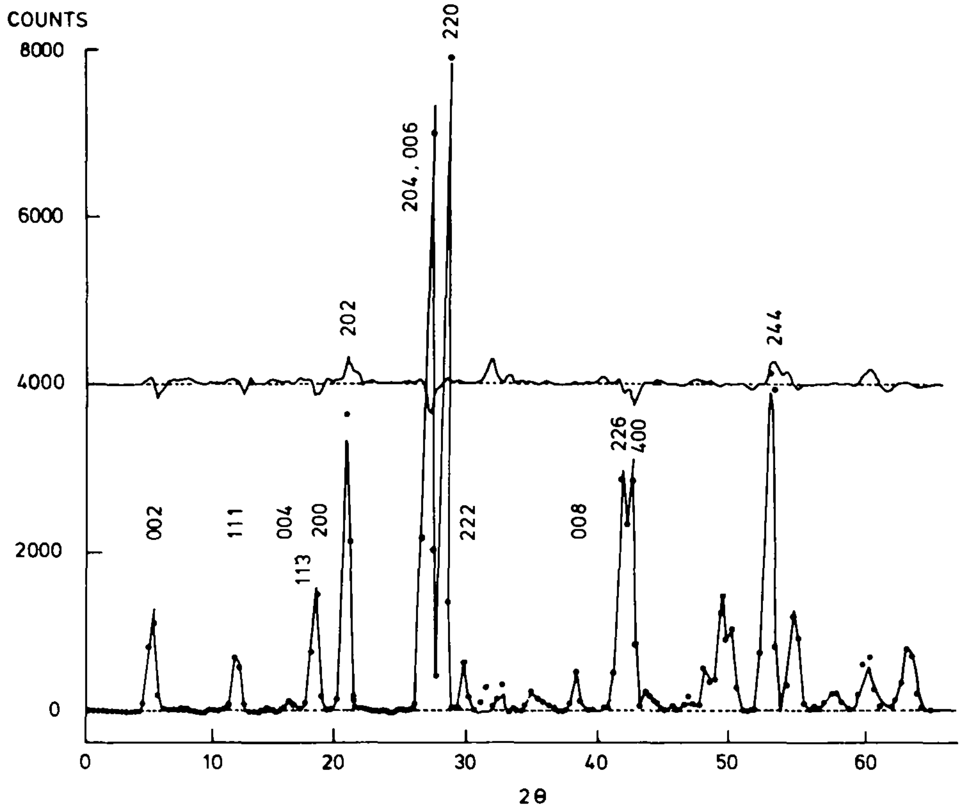

Figure 1. Powder neutron diffraction profile of Rb_2CrCl_4 at 4·2 K. The line through the data points is a fit to a model with the moment constrained along [010] (fit 2, table 1). The difference between observed and calculated profiles is indicated and major reflections are labelled.

indicates that the same final parameters, and insignificantly different R-values, are obtained if the moment direction is constrained to [100], thus confirming that the powder experiment is not sensitive enough to define the direction of the moment within the basal plane since the a and b parameters are almost identical.

However, if the moments are constrained to [001] R_p increases markedly, (fit 4) so that the data clearly indicate that the moments lie in the basal plane. In fact it is known from the single crystal neutron diffraction (Janke *et al* 1983) that the moments are aligned along ⟨100⟩.

The last two columns of table 1 list the parameters refined by Janke *et al* (1983) from single crystal neutron diffraction data at 78 K and 5·5 K. There is quite good agreement between the lattice constants and positional parameters obtained from both types of measurement. On the other hand, the Debye-Waller factors do not agree so well and for the powder data they have quite high standard deviations. The refined magnetic moment of 3·8(1) μ_B (fit 4) agrees reasonably well with the saturation value of 4·06(1) μ_B obtained from magnetization measurements (Cornelius *et al* 1986).

The magnetic and nuclear structure of a powder of composition $Rb_2Cr_{0.73}Mg_{0.27}Cl_4$ was refined in the same space group *Bbcm* setting the scattering length b at the Cr^{2+} site at $0{\cdot}73b_{Cr}+0{\cdot}27b_{Mg}$. The refined parameters are given in table 1 and the 4·2 K profile is shown in figure 2. It is worth noting that, in contrast to Rb_2CrCl_4, inclusion of the preferred orientation parameter has only a small effect on the R_p value, presumably because doping with Mg^{2+} makes the crystals harder to cleave. The magnetic moment of 2·5(3) μ_B (fit 5) agrees quite well with the value of 2·8 μ_B calculated as 73% of that of Rb_2CrCl_4. Constraining the moments to the [001] direction (fit 6) leads to an increase in R_M suggesting that the moments lie in the basal plane even in the Mg^{2+} doped compound. Doping with Mg^{2+} also increases the c lattice parameter but decreases a and b.

3.2 *Single crystal neutron diffraction: temperature dependence of (0, 0, 4)*

In a ferromagnetically ordered crystal the magnetic contribution to the neutron diffraction intensity is found at the same reciprocal lattice points as that arising from the nuclear scattering. Thus to follow the temperature dependence of magnetic intensity we must select a reflection with a favourable ratio of F_M to F_N. From our earlier single crystal neutron diffraction work on Rb_2CrCl_4 (Janke *et al*

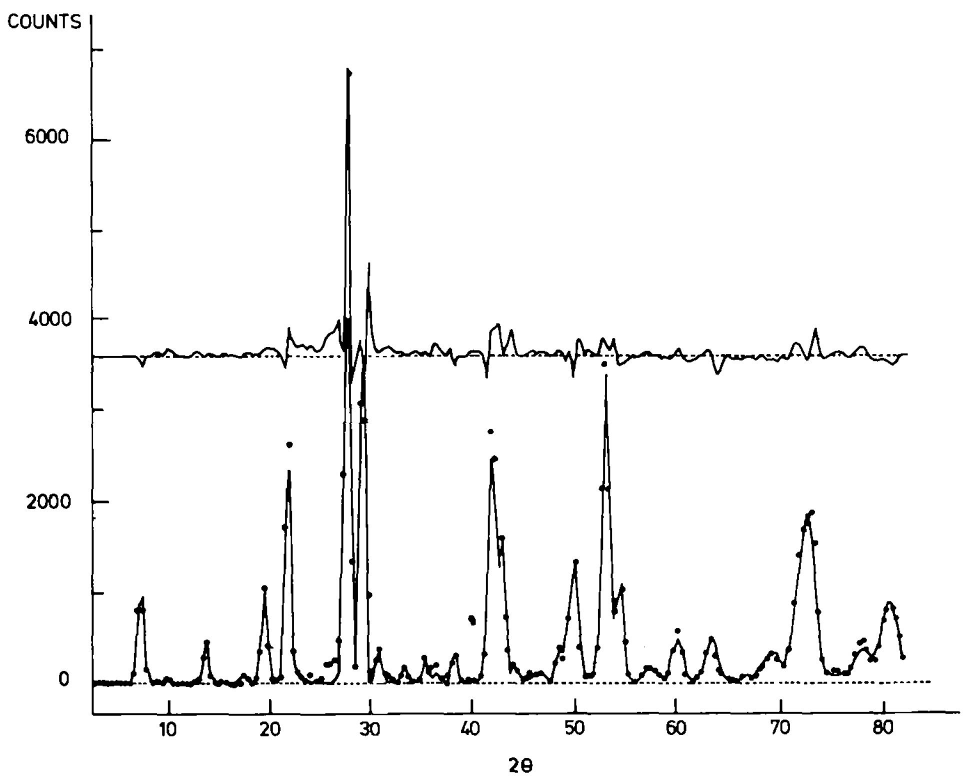

Figure 2. Powder neutron diffraction profile of $Rb_2Cr_{0.73}Mg_{0.27}Cl_4$ at 4·2 K. The line through the data points is a fit to a model with the moment along [010] (fit 5, table 1). The difference between observed and calculated profiles is indicated.

1983) it was known that the (0, 0, 4) reflection is suitable for this purpose. This arises in part from the fact that Rb_2CrCl_4 is an easy-plane system, so since the scattered intensity

$$I \propto F_N^2 + F_M^2 \sin^2 \alpha, \tag{9}$$

[cf. (1) and (3)] the scattering vector of (0, 0, 4) is perpendicular to the moment direction. It can also be seen from figure 1 that the nuclear intensity of this reflection is particularly small. From (4) the magnetic structure factor at a temperature T

$$F_M(T) \propto \sum_j \sum_q f_j \mu_{j,q}(T), \tag{10}$$

where $\mu_{j,q}(T)$ is the moment residing on the jth atom at the qth equivalent position which becomes zero at T_c.

Results of the measurements of the magnetization of $Rb_2Cr_{0\cdot89}Mg_{0\cdot11}Cl_4$ and $Rb_2Cr_{0\cdot97}V_{0\cdot03}Cl_4$ measured in this way are shown as a function of temperature in figure 3. From this figure we see that T_c of the Mg^{2+} doped crystal is 42 K, i.e. substituting 11% of the Cr^{2+} by Mg^{2+} decreases T_c by 10 K or 19%. A comparable proportional decrease in T_c has been found in $K_2Cu_xZn_{1-x}F_4$ (Okuda *et al* 1980) a two-dimensional $S = ½$ Heisenberg ferromagnet, for which single crystals could be grown at all concentrations from $x = 0$–1. In addition Kurtz (1982) studied the magnetic properties of $Rb_2Cr_xCd_{1-x}Cl_4$ by single crystal magnetometry, and found that in samples containing up to 14% Cd^{2+}, T_c decreased while the saturation moment per Cr^{2+} ion was the same as in Rb_2CrCl_4. On the latter point, our powder diffraction result for the 27% Mg^{2+}-substituted sample (§ 3.1) leads us to the same conclusion.

Our single crystal neutron diffraction measurements on the V^{2+}-doped crystal (figure 3) indicate T_c as 49·3 K, a value comparable with that observed in $Rb_2Cr_xMn_{1-x}Cl_4$ at similar values of x (Munninghoff *et al* 1981). In the latter the Mn^{2+}-Mn^{2+} and Mn^{2+}-Cr^{2+} exchange is antiferromagnetic and in contrast to the situation with Mg^{2+} doping, Munninghoff *et al* (1981) found that on diluting Rb_2CrCl_4 with Mn^{2+}, not only T_c but also the saturation moment per metal ion decreases.

3.3 *Optical absorption spectra: sidebands in* $Rb_2Cr_{0\cdot97}V_{0\cdot03}Cl_4$ *and* $Rb_2Cr_{0\cdot95}Fe_{0\cdot05}Cl_4$

Further evidence for the antiferromagnetic sign of the Cr^{2+}-Mn^{2+} exchange constant in Mn^{2+}-doped Rb_2CrCl_4 has come from studies of the optical absorption spectrum. Wood *et al* (1982) first observed satellite absorption bands near the 623 nm exciton-magnon combination band in Rb_2CrCl_4 crystals doped with Mn^{2+}. These extra bands were assigned as Cr^{2+} ligand field excitations, which take place with a decrease of spin, accompanied by spin flips on isolated Mn^{2+}, antiferromagnetically coupled to Cr^{2+} neighbours. The Cr^{2+} ground state is $^5B_{1g}$ and the Mn^{2+} is $^6A_{1g}$. Therefore the coupled ground state wavefunction of a Cr^{2+}, Mn^{2+} pair can be written $|G\rangle = |-5/2, 2\rangle = |M_S^{Mn^{2+}}, M_S^{Cr^{2+}}\rangle$ where M_S is the magnetic quantum number. Thus the first excited state is $|E_1\rangle = |-3/2, 1\rangle$, the second excited state is $|E_2\rangle = |-½, 0\rangle$ and so on.

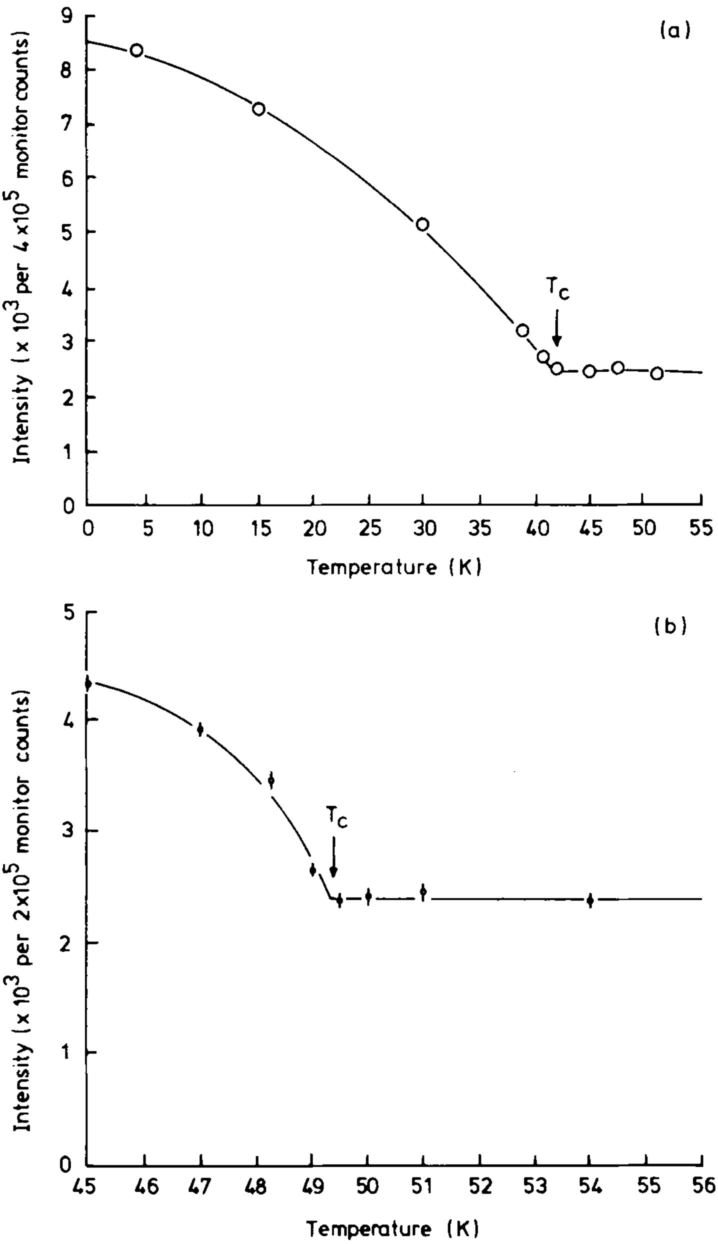

Figure 3. Temperature dependence of the peak intensity of (0, 0, 4) in the single crystal neutron diffraction of **(a)** $Rb_2Cr_{0\cdot89}Mg_{0\cdot11}Cl_4$ and **(b)** $Rb_2Cr_{0\cdot97}V_{0\cdot03}Cl_4$, corrected for diffuse scattering and background.

To confirm that the sidebands were caused by spin flips of the impurity ions coupled to Cr^{2+} excitons we measured the absorption spectrum of $Rb_2Cr_{0.95}Mg_{0.05}Cl_4$ since substitution of Cr^{2+} with non-magnetic ions should not introduce any sidebands. The axial absorption spectrum is shown in figure 4. The spectra are indeed identical to that of pure Rb_2CrCl_4, substantiating the coupled spin-flip mechanism for the Mn^{2+} doped compounds.

The effect on the absorption spectrum of doping transition metal cations other than Mn^{2+} can now be considered and V^{2+} (ground state ${}^4A_{2g}$) and Fe^{2+} (ground state ${}^5B_{1g}$) were chosen. The spectrum of $Rb_2Cr_{0.97}V_{0.03}Cl_4$ is shown in figure 4b. By comparison with figure 4a, which is the same as the spectra of undoped Rb_2CrCl_4, we see that in the V^{2+}-doped crystal there are two satellite bands between the major 6310 Å exciton-magnon bands. These satellite absorption bands, which we shall call a_1, a_2 etc. are similar to those observed in the Mn^{2+}-doped crystals. Following a similar molecular field argument to Wood *et al* (1982) the observations may be understood by considering an isolated V^{2+} or Fe^{2+} to interact via a Heisenberg exchange mechanism, with the surrounding Cr^{2+} represented by a molecular field.

With z taken to be the spin direction in ordered Rb_2CrCl_4 then

$$H = H_1 + H_2, \tag{11}$$

where

$$H_1 = -K_V S_z(V) - K_{Cr} S_z(Cr) - J_{CrV} S_z(V) \cdot S_z(Cr), \tag{12}$$

$$H_2 = J_{CrV}/2\{S_+(V)S_-(Cr) + S_-(V)S_+(Cr)\}, \tag{13}$$

K_m is the molecular field term around the ion M where K_V is negative and K_{Cr} is positive. J_{CrV} is the CrV exchange constant taken to be anti-ferromagnetic.

The ground state is represented as $|G\rangle = |-3/2, 2\rangle$ and the excited states are $|M_S(V), M'_S(Cr)\rangle$ where the prime notation indicates that Cr^{2+} is in its excited triplet state; a_1 is the transition to the first excited state $|-1/2, 1\rangle$, a_2 to the second excited state $|1/2, 0\rangle$ and a_3 to the third excited state $|3/2, -1\rangle$. The pure spin flip transition is to the excited state $|-3/2, -1\rangle$.

The excited state energies are given by

$$E(M_S(V), M'_S(Cr)) = -K_V M_S(V) - K'_{Cr} M'_S(Cr) - J' M_S(V) M'_S(Cr). \tag{14}$$

Therefore the successive energy intervals between the pure Cr spin-flip and a_1, a_2, a_3 are $(-K_V - J')$, $(-K_V + K'_{Cr} - 1/2J')$, $(-K_V + K'_{Cr} + 3/2\,J')$. If $|K_V|$ is assumed to be the dominant term (i.e. $J_{Cr'Cr}$ and J_{CrV} are small) the intervals are equal as observed. To obtain more precise estimates it will be necessary to measure the spectra at lower temperatures to remove the hot bands completely (Janke *et al* 1982). Now $|K_V|$, the molecular field term around V^{2+}, is given as follows:

$$|K_V| = 2ZSJ_{CrV} = 12J_{CrV}, \tag{15}$$

Thus from figure 4b the $a_2 - a_1$ interval is 53 cm^{-1}, leading to an estimate of J_{CrV} as $\sim 4{\cdot}4\ cm^{-1} \equiv 6{\cdot}3$ K from (15). Finally the absorption bands of $Rb_2Cr_{0.95}Fe_{0.05}Cl_4$ are shown in figure 4c, measured under the same conditions. By comparison with figure 4a there are at least two satellite bands in the 623–6310 Å region. Using the same arguments as in the V^{2+} case and (15) we find J_{CrFe} is 5·2 K.

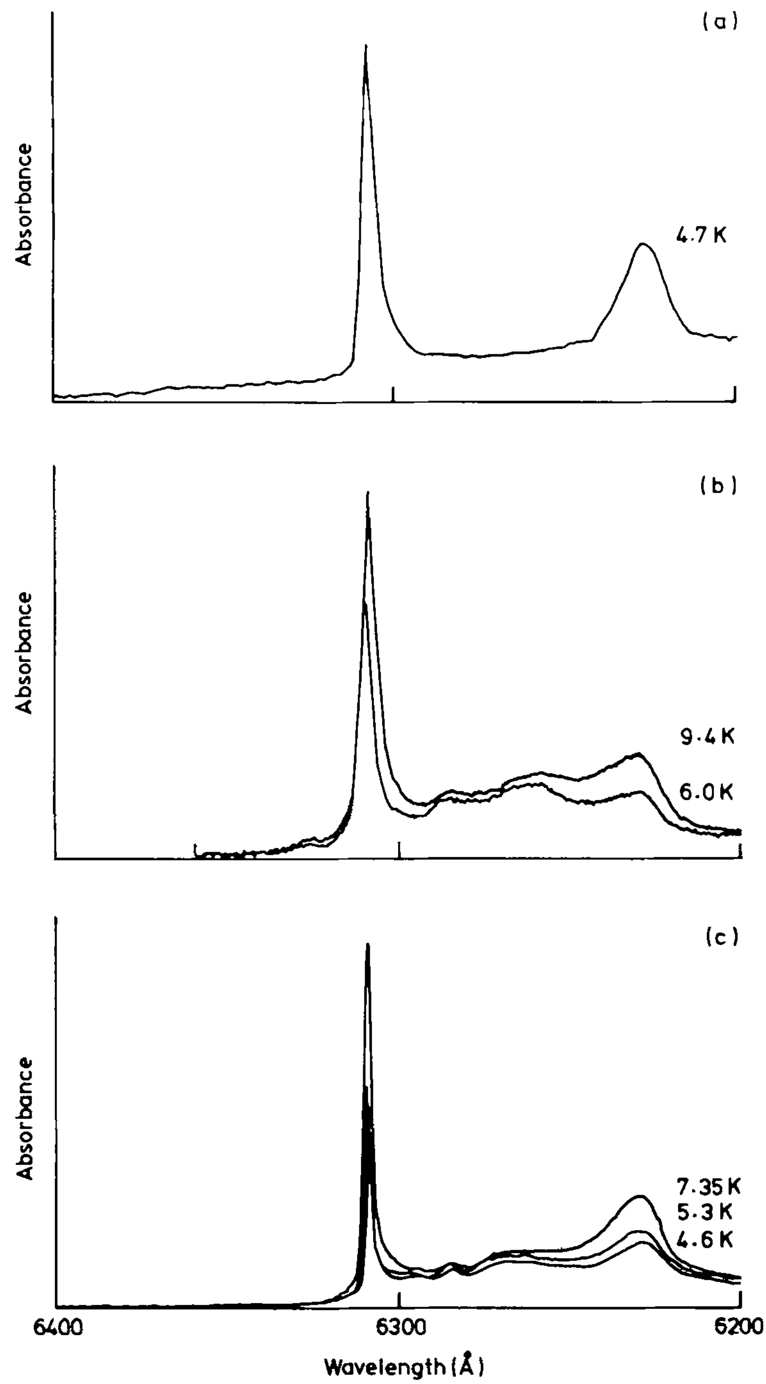

Figure 4. Axial absorption spectra of **(a)** $Rb_2Cr_{0.95}Mg_{0.05}Cl_4$, **(b)** $Rb_2Cr_{0.97}V_{0.03}Cl_4$ and **(c)** $Rb_2Cr_{0.95}Fe_{0.05}Cl_4$ at various temperatures.

4. Conclusions

We have shown how a combination of powder and single crystal neutron diffraction, together with optical spectroscopy, can illuminate the effect of doping either magnetic or non-magnetic cations substitutionally into the Cr^{2+} sites of the ionic ferromagnet Rb_2CrCl_4. Powder diffraction shows that with 27% Mg^{2+} substitution long range magnetic order persists at 4·2 K and the moments remain parallel to the basal plane. From single crystal diffraction we find that substitution of 11% Mg^{2+} lowers T_c by 19% while substitution of 3% V^{2+} lowers it by 6%. By examining the satellite bands which appear alongside the exciton-magnon hot bands in the visible absorption spectrum of Rb_2CrCl_4 when it is doped with small amounts of magnetic impurities, we have also estimated near-neighbour Cr^{2+}-V^{2+} and Cr^{2+}-Fe^{2+} exchange constants. Both are antiferromagnetic in sign and respectively 6·3 K and 5·2 K in magnitude. These figures are to be compared with 3·0 K for the Cr^{2+}-Mn^{2+} exchange constant in the same material.

Acknowledgement

We thank the S.E.R.C. and U.K.A.E.A. for supporting this work through a CASE Studentship and E.M.R. contract to P.J.F.

References

Bacon G E 1975 *Neutron diffraction* 3rd edn (Oxford: University Press)
Cornelius C A, Day P, Fyne P J, Hutchings M T and Walker P J 1986 *J. Phys.* **c19** 909
Halpern O and Johnson M H 1939 *Phys. Rev.* **55** 898
Harrop M C 1981 D.Phil. thesis Oxford University
Hutchings M T, Als-Nielsen J, Lindgard P A and Walker P J 1981 *J. Phys.* **c14** 5327
Janke E, Hutchings M T, Day P and Walker P J 1983 *J. Phys.* **c16** 5959
Janke E, Wood T E, Ironside C and Day P 1982 *J. Phys.* **c15** 3809
Kurtz W 1982 *Solid State Commun.* **42** 875
Munninghoff G, Kurtz W, Treutmann W, Hellner E, Heger G, Lehner N and Reinen D 1981 *Solid State Commun.* **40** S71
Okuda Y, Tohi Y, Yamada I and Haseda T 1980 *J. Phys. Soc. Jpn.* **49** 936
Rietveldt H M 1969 *J. Appl. Cryst.* **2** 65
Shante V K S and Kirkpatrick S 1971 *Adv. Phys.* **20** 235
Shinagawa K and Tanabe Y 1971 *J. Phys. Soc. Jpn.* **30** 1280
Walker P J, Wondre F and Fyne P J 1982 *J. Cryst. Growth* **60** 155
Wood T E, Cox P A, Day P and Walker P J 1982 *J. Phys.* **c15** L787